On the reduction of trend errors by the ANOVA joint correction scheme used in homogenization of climate station records

by

Ralf Lindau and Victor Venema

Meteorological Institute

University of Bonn

Auf dem Hügel 20

D 53121 Bonn

Germany

Correspondence to Ralf Lindau (rlindau@uni-bonn.de)

Short Title: ANOVA joint correction scheme

Keywords: Homogenization, climate stations, temperature trends, correction scheme, adjustment

Abstract. Inhomogeneities in climate data are the main source of uncertainty for secular warming estimates. To reduce the influence of inhomogeneities in station data statistical homogenization compares a candidate station to its neighbors to detect and correct artificial changes in the candidate. Many studies have quantified the performance of statistical break detection tests used in this comparison. Also full homogenization methods have been studied numerically, but correction methods by themselves have not been studied much. We analyze the so-called ANOVA joint correction method, which is expected to be the most accurate published method. We find that, if all breaks are known, this method produce unbiased trend estimates and that in this case the uncertainty in the trend estimates is not determined by the variance of the inhomogeneities, but by the variance of the weather and measurement noise. For low signal-to-noise ratios and high numbers of breaks, the correction may also worsen the data by increasing the original random unbiased trend error. Any uncertainty in the break dates leads to a systematic undercorrection of the trend errors and in this more realistic case the variance of the inhomogeneities is also important.

1 Introduction

The main obstacle to accurate long-term trend estimates is the presence of inhomogeneities that are hidden in the data (Parker 1994, Brohan et al., 2006, Aguilar et al., 2003, Menne et al., 2010, Brunetti et al., 2006, Begert et al., 2005, Auer et al., 2005). Important reasons for inhomogeneities are relocations of the stations and changes in their surroundings, as well as changes in the screens and instruments (Peterson et al., 1998).

Statistical homogenization algorithms aim at detecting and correcting these spurious effects by comparing a candidate station to its neighboring reference stations. All nearby stations are assumed to observe the same regional climate signal, while the perturbations due to inhomogeneities are assumed to be different for every station (Conrad and Pollak, 1950).

Previous studies have mostly focused on the accuracy of break detection (Easterling and Peterson, 1995; Ducré-Robitaille et al., 2003; DeGaetano, 2006; Beaulieu et al., 2008; Kuglitsch et al., 2012). More recent numerical validation studies looked at the performance of both the break detection and complete homogenization algorithms (Domonkos, 2008; Domonkos, 2011; Venema et al., 2012; Williams et al., 2012; Chimani et al., 2018; Killick, 2016). The HOME benchmarking study for European climate station networks found that the performance for break detection and trend accuracy were only modestly correlated (Venema et al., 2012). This implies that also the other components of homogenization methods, including break correction, are important.

The performance of correction methods has hardly been studied, but Domonkos et al. (2013) found that the *station* trends and RMSE of all contributions to the HOME benchmark that did not use the modern ANOVA joint correction model yet, were improved by applying this method.[1] The HOME benchmark did not have an explicit trend bias due to inhomogeneities, the small stochastic *network-wide* trend biases were hard to remove and the changes due to applying the ANOVA method more mixed (Domonkos et al., 2013).

[1] One contribution was made worse due to the application of the ANOVA method, likely because the information on the break positions contained errors.

In the HOME benchmark the error in the network temperature trends themselves were about halved by the best homogenization methods, while the error of the station trends were reduced to a quarter (Venema et al., 2012). The validation study of the Pairwise Homogenization Algorithm for US climate station network did add explicit network-wide temperature trend errors due to inhomogeneities (Williams et al., 2012). For the two most realistic scenarios the remaining network trend bias is a few percent to 20 percent. For the hardest (unrealistic) scenario with many small biased breaks about half of the trend bias remained. Both validation studies were for high-quality well-correlated networks. The median station trend error in the Austrian validation study for relative humidity station data could be reduced by a factor of 2 due to homogenization with ACMANT and HOMER (Chimani et al., 2018). The validation dataset did include an explicit trend error, but the relative humidity observations have very low correlations, the median correlation was only 0.7.

The original ANOVA method decomposes the observations of a set of climate stations into (1) a regional climate signal for all stations, (2) a break signal (step function) per station defined by the previously detected breakpoints and (3) noise (Caussinus and Mestre, 2004). The method minimizes the noise to estimate the common climate signal and the break signals. Domonkos (2017) improved this method by relaxing the assumption that all stations have the same climate signal by estimating the regional climate signal of the candidate as a squared-correlation weighted average. This gave small, but consistent improvements in his validation datasets of about 1 %; for sparse networks and regions where the regional climate changes considerably in space, such as the Arctic, this new method may give larger improvements.

This study sets out to study how accurately the ANOVA joint correction model can remove trend errors in station data. Because the description of the ANOVA model in Caussinus and Mestre (2004) was short, we will detail the method in Appendix A. In Section 2 on the methodology we explain how homogenization works and argue that the main task of homogenization is to get the network-wide trends right. It furthermore details how the study data was simulated and how we assess the performance of the correction algorithm.

We will analyze four scenarios: with and without a bias in the breaks that produces a systematic trend error and with and without errors in the positions (dates) of the breaks. The results for these scenarios are presented in Section 3.1 to 3.4. The simplest scenario of no bias and no position errors lends itself to a detailed mathematical analysis in Section 3.1 where we compare our theoretical expectation of input and output errors with our empirical findings. For a signal to noise ratio of one and six breaks in each time series the input and output errors for the network-wide trend are equally large, while the number of stations is less important (Section 3.1.2). For the more complex scenarios, which include also biased breaks, we show that an unbiased correction is possible if the break positions are exactly known, but that any trend bias is only partly corrected if the break positions are uncertain. The paper closes with a summary and discussions.

2 Methodology

Statistical homogenization algorithms consist of three parts, where the first is dedicated to detecting the break positions. For this purpose, differences with neighboring station are considered. In this way the natural variability is reduced, which would otherwise dominate the signal. Uncertainties occurring during the detection part are discussed in Lindau and Venema (2016). For pairwise methods the second step is called attribution. Here the decision is made, which of the involved stations is responsible for a detected break. Other algorithms avoid this step by using a composite reference of the surrounding network; the problem here is to produce a composite that is free of breaks. The third and last step is the correction. This step is the topic of this study. We concentrate on the so-called ANOVA correction method, which is described in detail in Appendix A.

This paper is focused on the ability to remove linear trend errors from the data. Trends can be computed separately for each station or as regional average over the entire network. Large-scale trends are climatologically more important than station trends. Moreover, there is a much easier way to estimate the station-to-station variability of trend errors directly from the data, without running a full homogenization algorithm. The trend TRD_i at a station i consists of two additive components, the spurious trend due to inhomogeneities B_i and the true climate trend C, which is the same for all stations of the network:

$$TRD_i = C + B_i \tag{1}$$

The average of all trend differences between a candidate station i_0 and its n neighbor stations i gives a direct estimate of the spurious break induced trend at the candidate station relative to the network mean.

$$\frac{1}{n}\sum_{i=1}^{n}(TRD_{i0} - TRD_i) \;=\; \frac{1}{n}\sum_{i=1}^{n}(C + B_{i0} - C - B_i) \;=\; B_{i0} - \frac{1}{n}\sum_{i=1}^{n} B_i \tag{2}$$

Thus, the trend error of each station B_{i0} is easily to infer, if the mean spurious trend of the entire network is known. Therefore, we focus on the latter, i.e. on regional averages of the inhomogeneity effects over several neighboring stations.

The default configuration to study the performance of the ANOVA correction scheme is to simulate data for 1000 networks consisting of n = 10 stations each. The length of each station time series is equal to m = 100 and consists of three superimposed signals.

1. The climate signal, which is identical for all stations of a network.
2. Noise added to the climate signal, which mimics the differences between the stations within a network, e.g., due to measurement errors and the weather.
3. Inhomogeneities inserted at random timings and with random strength.

All three signals are randomly chosen from a normal distribution with zero mean. The first one, i.e. the climate signal, can be seen as a sequence of 100 yearly means or alternatively as 100 January (or July) means, which is the typical format of temperature data to be homogenized. Such annual or monthly averages with 12 month time lag have only a low mutual dependence and can be well modelled by Gaussian white noise. The same is true for the other two signals, i.e. the noise part itself and the breaks (Menne et al., 2005). All three signals having zero mean is justified because the correction scheme is not able to make any statement about the overall temporal mean of each station (see Appendix A).

The three standard deviations are varied, but their default values are set to σ_c = 3 for the climate and to 1 for the noise variance σ_n^2 and break variance σ_b^2. All three are altered later in this study to analyze their impact on the performance of the correction scheme. This is also true for the number of breaks k, which we set to a default value of 5, according to the estimate of Venema et al. (2012)

for Europe. In the simulation, the break positions are determined by random numbers drawn from a uniform distribution. The first break has m-1 possible locations, the second m-2, etc. In this way we are able to create time series with exactly five breaks each.

After creation, the temporal average of each time series is set to zero. One reason is mentioned above: the correction cannot cope with mean differences between the stations. Additionally, we are aiming at trends and these are independent from the temporal mean at each station.

2.1 Skill Measures

As specified above, the simulated observations $O(i,j)$, given for each station i and year j, consist of three superimposed signals: The climate C, the weather W, and the inhomogeneities B (Eq. 3). We will show in the following that the climate signal, although it is in many cases the most interesting one, is cancelled out while running the correction scheme. The inhomogeneities are the signal that has to be detected, isolated and suppressed. The weather acts as noise hampering the estimation of the break signal. Therefore, weather and noise are used in the following as synonyms.

$$O(i,j) = C(j) + W(i,j) + B(i,j) \tag{3}$$

We are searching for the truth T, i. e. the observations without the inhomogeneity signal:

$$T(i,j) = C(j) + W(i,j) \tag{4}$$

The correction scheme provides us with the detected inhomogeneity signal D and the correction is actually performed by subtracting D from O. Thus, the homogenized data H is:

$$H(i,j) \;=\; O(i,j) - D(i,j) \;=\; C(j) + W(i,j) + \underbrace{B(i,j) - D(i,j)}_{R(i,j)} \tag{5}$$

The most intuitive skill measure is probably the detected inhomogeneity D:

$$D(i,j) \;=\; O(i,j) - H(i,j) \tag{6a}$$

In Eq. (5) the remaining inhomogeneity signal R occurs, which is in general not zero, because the correction scheme will not be perfect. Inserting Eq. (4) into (3) and (5) we get for the deviations from the truth:

$$B(i,j) = O(i,j) - T(i,j) \tag{6b}$$

$$R(i,j) = H(i,j) - T(i,j) \tag{6c}$$

Eq. (6a-c) give the three parameters used to estimate the skill of the correction procedure. B is giving the deviation from the truth before the homogenization, whereas R is the deviation after the homogenization. We denote B as inserted or input error, D as detected error, and R as remaining or output error. Two skill measures are used:

Measure 1: Comparison of inserted error B and detected error D
Measure 2: Comparison of inserted error B and remaining error R

The comparison is performed in the following by scatterplots, where the key parameters are the means, the variances, and the correlation between B and D, and between B and R, respectively.

2.2 Analyzed three steps

The main aim of this study is to analyze the ability of the ANOVA correction scheme to improve the estimates for the network-mean trends. This total process can decomposed into three parts.

Step 1: The correction itself, i.e. the determination of the inhomogeneities
Step 2: The resulting correction of the trend for each station separately.
Step 3: The effect of averaging the 10 station trends of each network.

Although our focus is assessing the skill of the entire three-step process as whole, i.e. which effect do inserted inhomogeneities have on the network mean trend, it helps our understanding to also show intermediate products after step 1 and 2.

2.3 Analyzed scenarios

In the main scenario we (1) insert breaks with zero mean and (2) use the correct break positions within the ANOVA correction scheme. These two characteristics are then separately changed to biased breaks (with non-zero mean) and perturbed (intentionally worsened) break positions, so that four scenarios result:

Scenario 1: Zero mean (unbiased) breaks together with correct break positions
Scenario 2: Non-zero mean (biased) breaks together with correct break positions
Scenario 3: Zero mean (unbiased) breaks together with perturbed break positions
Scenario 4: Non-zero mean (biased) breaks together with perturbed break positions

Zero-mean breaks introduce false trends for each station and hence also a (reduced, but remaining) error for the entire network. However, on average there will be no mean trend error, but only an increased random scatter of the individual network trends. This will be different when biased (non-zero) breaks are inserted in (Scenarios 2 and 4). In these cases an overall effect of the breaks on the trend is expected.

In our study the correct break positions are known, because we use artificial data. Since we focus on the last step of the homogenization procedure, the correction itself, it is justified to use these true breakpoint positions to isolate the performance of the correction scheme alone. However, in reality the break positions will not be perfectly determined. The additional impact of these position errors are analyzed in scenario 3 and 4, by adding random perturbations to the true break positions. A summary of the main experiments is given in Tab. 1.

3 Results

3.1 Scenario 1: unbiased breaks, correct break positions

In this scenario we assume both no overall trend bias and perfect break detection. The first study is very simplistic: We set the noise to zero and check the result after step 1. Fig. 1 shows the inserted inhomogeneities for each year, station, and network on the abscissa against the output of the correction scheme on the ordinate. Actually, 1,000,000 crosses should appear, but for technical reasons we displayed only a subset. However, the statistics is based on the full dataset. The test yields a perfect correlation between the input inhomogeneities and the detected ones. Thus, the correction scheme works perfectly, if no noise between the stations is present and if the break positions are known. The perfect result is not completely trivial, as only the break positions, but not their sizes are used as input of the algorithm.

We repeat this study with different values for σ_c and found no differences in the result. This is expected. In the correction scheme, only differences of overlapping time periods between two stations of the same network are considered (Appendix A). Consequently, the climate signal, which is assumed to be the same at every station of a network, is completely cancelled out. Thus, the climate signal, while always generated in our simulations, is not relevant and not further considered.

The second study is conducted with non-vanishing noise variance $\sigma_n^2 = 1$. In Fig. 2 the results for all three processing steps (as defined in section 2.2) are presented. The three panels show on the x-axis the inserted quantity and on the y-axis the detected one (i.e. Measure 1). In Fig. 2a the situation after applying the correction scheme is shown. Both means are zero, the detected variance is with 0.786 slightly higher than that for the inserted one (0.719). The correlation remains rather large with 0.955. In Fig. 2b the resulting linear station trends (for 10 station times 1000 networks) are given. These trends are calculated by linear least squares regression. Temperature trends normally have the dimension "Kelvin per time". However, here we multiplied it with the total length of the time series so that the trend expresses the total temperature change during the considered time period (explainable by a linear trend). Compared to Fig. 2a, the variances of input and output both increase by a factor of about 3, while the correlation is only slightly decreased. In the third step the 10 station trends of each network are averaged. By the averaging process the variances are both reduced, but that of the detected trend less than that of the input. The correlation decreases to 0.812.

Additionally, the two regression lines (one with assuming *x* and one with assuming *y* as independent variable) are given. A striking feature in all three scatterplots is that the regression line of *y* on *x* falls together with the 1-to-1 line for *x* = *y*. This characteristic occurs, if *y* is equal to *x* plus a random scatter variable ε.

$$y_j = x_j + \varepsilon_j \tag{7}$$

If Eq. (7) is true, the slope *a* of the regression line is equal to 1. A short rational is given by the following equation chain, where we used Eq. (7) at the forth equal sign:

$$a = r\frac{\sigma_y}{\sigma_x} = \frac{cov}{{\sigma_x}^2} = \frac{\sum_{i=1}^{n} x_i y_i}{\sum_{i=1}^{n} {x_i}^2} = \frac{\sum_{i=1}^{n} x_i (x_i + \varepsilon_i)}{\sum_{i=1}^{n} {x_i}^2} = \frac{\sum_{i=1}^{n} {x_i}^2}{\sum_{i=1}^{n} {x_i}^2} = 1 \tag{8}$$

where two variables *x* and *y* comprising *n* values with zero mean are considered. The terms *r* and *cov* denote their correlation and covariance, respectively. The standard deviations are referred to as σ_y and σ_x.

For the above discussed reason, it is convenient to display not *y* (the detected error *D*), but the difference *x-y* (the remaining error *R*) on the ordinate (Fig 3). The correlation is negligible in all cases, which confirms that Eq. (7) is valid here. The variable on the x-axis (the inserted error *B*) is unchanged compared to Fig. 2 so that its statistics remains of course the same. The key parameters are the variances of inserted and remaining quantities *B* and *R*.

Fig. 3c shows an inserted network-mean trend variance of 0.265, the remaining one after correction is smaller with 0.133, but in the same order of magnitude. On both axes, we consider trends of inhomogeneities and no real climate trends. Therefore, we are dealing with the uncertainty introduced by the inhomogeneities on the trends. The interpretation of the found numbers is as following. If both the standard deviation of noise and that of breaks are equal to 1 K, the existing inhomogeneities make it a priori rather difficult to determine the network-mean trend accurately. The x-axis variance can be referred to as the input trend error variance, and its square root is as large as f = 0.515 K. Thus, the secular trend of this small network is in same order of magnitude as the climate trend itself. The y-axis variance can be interpreted as output trend error variance. The corresponding uncertainty of the network mean trend after correction is with g = 0.365 K comparable in size.

In the first study (Fig. 1), we have shown already that the climate signal is irrelevant for the correction and that it works perfectly under the absence of noise. From this, it is obvious that the output error R depends only on the noise variance. The input error is nothing else than the trend inserted by inhomogeneities. Therefore, it is clear that the input error depends only on the break variance.

However, to show it formally, we vary the noise and break variance in the next test. First the standard deviation of the inserted breaks is increased to σ_b = 2 (with σ_n = 1). As consequence, the input error increases by a factor of 2, while the output error remains unchanged (Fig. 4). If vice versa the noise is set to σ_n = 2 (with σ_b = 1), the output error is doubled, while no change in the input error is observed (Table 1). Further studies with various combinations of σ_b and σ_n confirm that i) the input error depends only on the break variance and the output error only on the noise variance and that ii) the relationships are both linear.

Consequently, we have two separated processes as illustrated by the flowchart given in Fig. 5. On the one hand, there is the conversion chain from the initial break variance (state in0) down to the error variance of the inserted network trends (state in3). On the other hand there is the transformation from the initial noise variance (state out0) down to the error variance of the remaining network trends (state out3). The first conversion chain considers input parameters beginning with the break variance σ_b^2 and ending with the trend variability before the correction σ_{in}^2. The second chain deals with output parameters. It starts from the noise variance σ_n^2, which finally defines the remaining trend variability σ_{out}^2 after the correction. Three factors for each chain, f_1^2 to f_3^2 and g_1^2 to g_3^2, denote the conversions of the variances from step to step. The total conversion factors are given by the product of the three partial factors:

$$f^2 = f_1{}^2 \times f_2{}^2 \times f_3{}^2 \qquad (9a)$$

$$g^2 = g_1{}^2 \times g_2{}^2 \times g_3{}^2 \qquad (9b)$$

Let us first consider the numerical values of the factors f^2 and g^2 as whole and coming to the detailed analysis of the partial factors later in Section 3.1.1. In our experiments we set the initial variances σ_b^2 and σ_n^2 to 1 so that the factors f^2 and g^2 are directly visible as the two variances in Fig. 3c, which are 0.265 for the input and 0.133 for the output. Their square roots give the conversion factor for the standard deviation, which describe the errors.

Thus, in this case the input error σ_{in} and the output error σ_{out} defined as the initial and the remaining standard deviation of the network-mean trend are given by:

$$\sigma_{in} = f\,\sigma_b \qquad with\, f = \sqrt{0.265} = 0.515 \tag{10}$$

$$\sigma_{out} = g\,\sigma_n \qquad with\, g = \sqrt{0.133} = 0.365 \tag{11}$$

The fraction of input and output error is then:

$$\frac{\sigma_{in}}{\sigma_{out}} = \frac{f\,\sigma_b}{g\,\sigma_n} = \frac{f}{g}\,SNR \tag{12}$$

with SNR denoting the signal-to-noise ratio of the analyzed data. From Eq. (12) we see that, for the considered settings, the error is enlarged by the correction, if SNR < g/f = 0.71.

3.1.1 Theoretical considerations for the factors *f* and *g*

In the following we will estimate the factors f and g theoretically to confirm their numerical values determined so far only empirically (Eqs. (10) and (11)). First, we estimate the input factor f by considering the partial factors f_1 to f_3. It is based on σ_b, the standard deviation of the break signal.

Fig. 2a shows that the variance is reduced from state in0 to in1 by a factor of f_1^2 = 0.719. The numerical value of f_1^2 is discussed in the following. Each of the simulated time series contain five breaks, i.e. a step function with six subperiods of arbitrary lengths. Their step heights are chosen from a standard normal distribution. As mentioned above, we decided to set the mean of each of these simulated time series to zero. Hereby, a fraction of $1/m_{in}$ of the input variance is lost, where m_{in} is defined as the number of independents. In our case, a rough estimate is m_{in} = 6, as this is the number of subperiods. However, the subperiods have different lengths and this reduces the effective number of independents. A time series with one long and 5 very short subperiods will behave more as if it contains only one rather than 6 independents.

Thus, from the obtained variance of inserted inhomogeneities (0.719), we can conclude that the effective number of independents must be approximately 3.5, because:

$$f_1^{\,2} = 1 - \frac{1}{m_{in}} \cong 0.719 \quad \Rightarrow \quad m_{in} \cong 3.5 \tag{13}$$

In Appendix B we show that a good approximation for m_{in} is:

$$m_{in} = \frac{k}{2} + 1 \tag{14}$$

where k is the number of breaks. As we applied k = 5 in the simulation, Eqs. (13) and (14) are in good agreement.

In step 2 (from state in_1 to in_2), the transition from the variance of the inserted inhomogeneities (Fig. 3a) to the error variance of the inserted trend (Fig. 3b) is made. The trend is equal to the slope of the regression line and its error variance $\sigma_{slp}^{\,2}$ is:

$$\sigma_{slp}{}^2 = \frac{\sigma_y{}^2(1-r^2)}{\sigma_x{}^2(m_{in}-2)} \cong \frac{\sigma_y{}^2}{\sigma_x{}^2 m_{in}} = \frac{\sigma_y{}^2}{\frac{P^2}{12} m_{in}} \tag{15}$$

where $\sigma_y{}^2(1-r^2)$ denotes the variance unexplained by the trend, $\sigma_x{}^2$ the variance of the entire considered time period P, and m_{in} the number of independent observations. The approximation made in Eq. (15), is essentially justified because the trend typically explains only a small part of the total variance; and neglecting the small part it explains anyhow is further compensated by replacing the term $m_{in} - 2$ by m_{in}. In this study we treat trends as temperature changes over the entire period. Accordingly, errors of the trend are given by the product $P\sigma_{slp}$ so that the factor $f_2{}^2$ is given by:

$$f_2{}^2 = \frac{\left(P\sigma_{slp}\right)^2}{\sigma_y{}^2} \cong \frac{12}{m_{in}} \tag{16}$$

With $m_{in} = 3.5$ it follows a theoretical estimate of $f_2{}^2 = 3.4$. This value is nearly perfectly obtained in the simulation (the quotient of input variances in Fig. 3a and 3b is 2.354/0.719 = 3.3).

In step 3 (from state in_2 to in_3), the 10 station trends of each network are averaged. As they can be regarded as independent, we expect a variance reduction by a factor of 10. The transition from Fig. 3b (with an input variance of 2.354) to Fig. 3c (with an input variance of 0.265) confirms this approximately.

In three steps, we have retraced the development of the input error variance $\sigma_{in}{}^2$ beginning with the initial break variance $\sigma_b{}^2$. As these are connected by the factor f^2 (Eq. 9a), we have implicitly deduced a more general estimate for f^2:

$$\begin{aligned} f^2 = f^2(k,n) = f_1{}^2(k)\ f_2{}^2(k)\ f_3{}^2(n) &= \frac{m_{in}-1}{m_{in}}\frac{12}{m_{in}}\frac{1}{n} \\ &= \frac{\frac{k}{2}}{\frac{k}{2}+1}\ \frac{12}{\frac{k}{2}+1}\ \frac{1}{n} = \frac{24\,k}{n\,(k+2)^2} \end{aligned} \tag{17}$$

In the following the factor g is discussed. This is more complicated as here the matrix solving process performed within the correction scheme has to be considered. We start with the noise variance $\sigma_n{}^2$, which triggers errors in the determination of the inhomogeneities in the correction scheme. In Appendix A, we show that an estimate for the error variance of the inhomogeneities for known break positions is $k\,\sigma_n{}^2/(m-1)$. In our case with $k = 5$, $\sigma_n{}^2 = 1$, and $m = 100$, this is equal to about 0.05. The simulation in Fig. 3a shows an only slightly larger variance of 0.069, which roughly confirms our theoretical estimation. The transition from this initial variance (state out1) to the station trends variance (state out2) performs rather similar as found for the respective input parameters. The comparison of Fig. 3a and 3b shows that the obtained trend variance is again larger by a factor of about 3.35 (from 0.069 to 0.231). However, in the next step, that from station (state out2) to network trends (state out3), the output error variances behave rather different. They are only reduced from 0.231 to 0.133. Although we averaged again over 10 stations, the variance is only reduced by a factor of less than 2. The reason is that the used correction scheme is a regression method and such methods have the general property of producing depend solutions. The 10 station trends in each network are highly correlated. Consequently, we are not able to reduce the uncertainty significantly by averaging.

An exact equation for g^2 (analogue to Eq. 17) is difficult to give here. However, g^2 consists analogously of three sub-factors. The first one, g_1^2, determines the variance of inhomogeneities, and is in the order of 10 times smaller than f_1^2, because $(m_{in} - 1)/m_{in}$ is in the order of 1 and $k/(m\text{-}1)$ is in the order of 1/10. The transition to station trends (f_2^2 and g_2^2, respectively) is similar for input and output quantities. For the third factor the circumstances are reversed: The variance reduction for the output g_3^2 is in the order of 1, whereas that of the input f_3^2 is $1/n$, thus 10 times smaller. Consequently, the entire effect of all three sub-factors together is comparable. And this is the reason why *f* and *g* have the same order of magnitude for $m = 100$, $k = 5$, and $n = 10$.

3.1.2 The variation of the factors f and g with break and station numbers

However, both factors *f* and *g* are expected to depend on the number of breaks *k* and the number of stations *n*. We performed a fourth study and varied both, the number of breaks *k* between 2 and 9, and the number of stations *n* between 5 and 10. Fig. 6a shows the result for the factor *f*, which gives the translation factor from the standard deviation of the break heights to the resulting error of the network trend before correction. For the studied *k*-*n* combinations, *f* varies between 0.41 and 0.74. For *f*(5,10) we obtained 0.50. The slight difference to Eq. (10) (giving 0.51) is within the noise. Isolines are drawn for the obtained values, which indicate the growth of *f* with decreasing break and station number, respectively. The theoretical estimate from Eq. (17) is given by the fat isolines. It shows that theory and numerical results are in good agreement.

Fig. 6b gives the corresponding result for the factor *g*. It grows with increasing number of breaks, because the underlying uncertainties of the inhomogeneities do so. The dependence on the number of stations is, at least for small break numbers, less important. Fig. 6c shows the *k*-*n* dependence of the ratio *g*/*f*. Here, the dependence on break number dominates by far; the dependence on station number, which is found for the two factors separately, is largely cancelled out. The ratio *g*/*f* grows rather linearly with *k* and can be approximated by:

$$\frac{g}{f} = \frac{k}{6} \tag{18}$$

Inserting Eq. (18) into Eq. (12), we find:

$$\frac{\sigma_{in}}{\sigma_{out}} = \frac{6}{k} SNR \tag{19}$$

If the SNR is smaller than *k*/6 the output error is larger than the input error, which means that the correction scheme makes the trend uncertainty larger.

In Fig. 3c we compared the trend uncertainties of the uncorrected and corrected data. The correction procedure replaces the initial error of a certain network by a different one, which is uncorrelated ($r = 0.02$) and smaller, but comparable in size. Eq. (19) defines the threshold when it will become larger. However, already below this threshold the corrections produce dependent solutions within each network. But independence is an important feature in data analysis and homogenized data may not be useful whenever variability shall be investigated.

3.2 Biased breaks, correct break positions

So far, we did not take into account that the inhomogeneities may have a mean network-wide non-zero trend. Such an effect may occur in reality, for example, for a transition to Stevenson screens or due to the introduction of new instruments. To simulate this situation we add a fourth signal to the artificial data. The homogeneous subperiods of the break signal are shifted by ΔB upward or downward depending on the middlemost year j_m of the subperiod. Early inhomogeneities are shifted downward, late ones upward. In this way, a global mean trend bias is inserted into the data.

$$\Delta B = 0.01\,(\,j_m - 50.5) \tag{20}$$

where the middlemost year j_m may vary between 1 and 100. By applying Eq. (20), one may expect a resulting trend bias of 1K/cty. However, edge effects lead to a reduced linear trend bias so that only 0.897 K/cty is resulting (Fig. 7, fat line). Nevertheless, the inserted inhomogeneities still consist of two components: the discussed bias plus a random component. The latter adds noise to the data, which leads to random variations of the mean inhomogeneities and therefore to an uncertainty of the actually inserted trend bias. Fig. 7 (crosses) shows the resulting mean situation for all inhomogeneities. The actually inserted mean trend is slightly different with 0.873 K/cty.

The important question is of course, whether the correction scheme is able to identify and remove this mean trend bias. Fig. 8 shows that the answer is yes. The artificial systematic trend of 0.873 K/cty is almost entirely removed. The mean remaining trend error is as small as 0.001 K/cty. A comparison of Fig. 8 with Fig. 3c, where no trend bias exists, shows that the variation of individual network trend errors remains the same on both axes. The data cloud in Fig. 8 is solely shifted to the right on the abscissa. Thus, the uncertainty to determine an individual network trend is still high, but the important issue is the successful removal of the trend bias.

3.3 Unbiased breaks, scattered break positions

Up to now, we used the known break positions of the simulated data assuming hereby perfect break detection. In the following, we use slightly scattered break positions as a simple way to study the effect of unavoidable errors. For this purpose, the true break positions are shifted by random time spans based on Gaussian noise of a certain standard deviation σ_s. To conserve the original number of inserted breaks (five), we mirror any shift that would land outside the allowed time period (1 to 100). Fig. 9 shows the result for σ_s = 1. Please note that the chosen strength of scatter is still moderate: about 40% of the positions are in this case not altered at all, and about 50% are shifted by plus or minus one temporal item. The main effect of the now included break position errors is that input errors *B* on the abscissa and output errors on the ordinate are slightly correlated (please compare Figs. 3c and 9). Assuming error-free break positions *D* and *R* were uncorrelated, while their correlation is now equal to *r* = 0.143. Additionally, the output error is slightly increased from 0.133 to 0.162. In a further experiment, we doubled the break position errors to a standard deviation of 2

(Table 1). In this case the correlation is increased from r = 0.143 to r = 0.218. The correlations found between inserted and remaining errors show that the errors are only partly corrected.

3.4 Biased breaks, scattered break positions

Finally, we considered both together biased break sizes and scattered break positions. Fig. 10 shows again the scatterplot for inserted and remaining network trend errors for σ_s = 1. However, now the inserted breaks are additionally biased. Thus, concerning the effect of the bias Fig. 8 is the appropriate reference, while it is Fig. 9 for the effects of the position errors. Concerning the latter, input and output errors are again correlated with r = 0.147, which is rather similar to Fig. 9, where we found r = 0.143. However, more important is the ability of the correction scheme to remove overall trend biases. While it was possible to correct the trend bias nearly entirely, when the break positions are exactly known (Fig. 8), the mean trend bias of 0.873 K is now removed only partly (Fig. 10), 0.093 K (about 11%) remains. Increasing σ_s to 2 (Table 1) provides an almost doubled remaining bias (0.180 K = 21%).

4 Summary and Discussion

The performance of the so-called ANOVA correction method is studied with simulated data. A reasonable skill measure is the improvement compared to uncorrected data. Therefore, also the input errors, which are caused by the inhomogeneities, have to be quantified. We divide this break signal into a random part, characterized by the break variance (exclusively considered in scenarios 1 and 3), and a deterministic part, the trend bias, which is a constant non-zero trend in all time series (additionally considered in scenarios 2 and 4). Obviously, the latter is really harmful as it would falsify the mean trend, whereas the first merely increases the uncertainty.

For the output side, we showed that, apart from the number of breaks, two parameters are essential. First the noise (weather) variance, being the difference between the true station signal and the regional climate signal (Eq. (4)); and second the break position errors that may occur in the preceding detection part of the homogenization algorithm. Note, that the climate signal itself is completely canceled out by the correction method and has no influence on the result.

In the basic scenario we assumed perfect detection and no trend bias. In this simplistic case only the break variance (on the input side) and the noise variance (on the output side) plays a role, when the number of breaks is held constant. We showed that the input error depends only on the break variance, while the output error depends only on the noise variance. Input and output errors are independent from each other, both with zero mean. Thus, the breaks introduce an unbiased random trend error to each network and the homogenization replaces this input error by a different and independent, but also random and unbiased error after the homogenization process. The strength of this output error depends on the noise. For the basic scenario we showed that under realistic circumstances, i. e. six breaks in each station time series and a signal-to-noise ratio of 1, input and output trend uncertainties are equally large. If the noise becomes larger than the break variance (SNR < 1) and/or more than 6 breaks are hidden in the time series, the homogenization may also worsen the data by increasing the original random unbiased trend error.

Moreover, after correction the trend errors for the different stations of a network are mutually dependent. Statistical analyses based on these homogenized station data, which mistakenly assume independence, may conclude that false trends are significant, because they vary so little.

In this study we assumed that the breaks are noisy deviations from a baseline. However, many homogenization studies have assumed that the break signal is a random walk. Reality seems to lie in the middle for European networks (Venema et al., 2012). For the same break size distribution a random walk signal has a larger total variance. It could thus be that the above numbers are somewhat different for a random walk.

However, the strength of the ANOVA method became apparent, when we added a trend bias to the input data. An important finding is that a trend bias is almost perfectly corrected if the break positions are known. As mentioned above, the correction of possible trend biases is very important.

The focus of the study is the performance of the correction method in case of perfect knowledge about the breaks, but in practice the derived breaks will have flaws as well. In future it will be worthwhile to study the interactions between detection and correction in detail. To get a first glimpse of how the ANOVA method handles errors in the breaks we considered the impact of position errors in the input of the correction scheme. In a more realistic scenario the position error would be a function of break size (Lindau and Venema, 2016) and there would be missing and spurious breaks.

As expected for a regression method, the ANOVA method is only able to correct a part of the trend bias. For moderate perturbations of the break positions (σ_s = 2 time steps), 21% of the introduced trend bias remained in the corrected data.

In the real world, the break detection will not be perfect so that position errors are unavoidable. Consequently, we expect that any trend correction performed so far tends to be underestimated. This fits to the results of the validation study for the US network by Williams et al. (2012), where the algorithm was able to reduce trend errors, but some trend bias remained. In the most difficult case with 10 breaks per century half of the trend error remained. Formulated positively, also for this very difficult case homogenization was able to reduce the large-scale trend bias.

The correct climate trend for each network is a byproduct of the ANOVA decomposition. For users who are exclusively interested in this specific parameter, it would be appropriate to deliver these data directly. The detour over the determination of the inhomogeneities, the correction of the station data, the calculation of the station trends from this corrected data, and the final averaging over all stations of network could be avoided.

Acknowledgements

This study was supported by the German Science Foundation, by the grants LI 2830/1-1 and VE 366/8.

References

Aguilar E, Auer I, Brunet M, Peterson TC, and Wieringa J. 2003. Guidelines on climate metadata and homogenization. World Meteorological Organization, WMO-TD No. 1186, WCDMP No. 53, Geneva, Switzerland, 55pp.

Auchmann R and Brönnimann S. 2012. A physics-based correction model for homogenizing sub-daily temperature series. J. Geophys. Res., 117: D17119, doi: 10.1029/2012JD018067.

Auer I, Böhm R, Jurkovic A, Orlik A, Potzmann R, Schöner W, Ungersböck M, Brunetti M, Nanni T, Maugeri M, Briffa K, Jones P, Efthymiadis D, Mestre O, Moisselin J-M, Begert M, Brazdil R, Bochnicek O, Cegnar T, Gajic-Capka M, Zaninovic K, Majstorovicp Z, Szalai S, Szentimrey T, and Mercalli L. 2005. A new instrumental precipitation dataset for the Greater Alpine Region for the period 1800–2002, Int. J. Climatol., 25: 139–166.

Beaulieu C, Seidou O, Ouarda TBMJ, Zhang X, Boulet G, and Yagouti A. 2008. Intercomparison of homogenization techniques for precipitation data, Water Resour. Res., 44: W02425, doi: 10.1029/2006WR005615.

Begert M, Schlegel T, and Kirchhofer W. 2005. Homogeneous temperature and precipitation series of Switzerland from 1864 to 2000. Int. J. Climatol., 25: 65–80.

Brohan P, Kennedy JJ, Harris I, Tett SFB, and Jones PD. 2006. Uncertainty estimates in regional and global observed temperature changes: A new data set from 1850. J. Geophys. Res., 111: D12106, doi: 10.1029/2005JD006548.

Brunetti M, Maugeri M, Monti F, and Nanni T. 2006. Temperature and precipitation variability in Italy in the last two centuries from homogenized instrumental time series, Int. J. Climatol., 26: 345–381.

Caussinus H and Mestre O. 2004. Detection and correction of artificial shifts in climate series. J. Roy. Stat. Soc. C, 53: 405-425. doi: 10.1111/j.1467-9876.2004.05155.x.

Chimani B, Venema V, Lexer A, Andre K, Auer I, Nemec J. 2018. Intercomparison of methods to homogenise daily relative humidity. International Journal of Climatology, in press, doi: 10.1002/joc.5488.

Conrad V and Pollak C. 1950. Methods in climatology. Harvard University Press, Cambridge, MA, 459 pp.

DeGaetano AT. 2006. Attributes of several methods for detecting discontinuities in mean temperature series, J. Climate, 19: 838–853.

Domonkos P. 2008. Testing of homogenisation methods: purposes, tools and problems of implementation. Proceedings of the 5th Seminar and Quality Control in Climatological Databases, edited by: Lakatos M, Szentimrey T, Bihari Z, and Szalai S. WCDMPNo. 71, WMO/TD-NO. 1493: 126–145.

Domonkos P. 2011. Efficiency evaluation for detecting inhomogeneities by objective homogenization methods. Theor. Appl. Climatol., 105: 455–467, doi: 10.1007/s00704-011-0399-7.

Domonkos P. 2017. Time series homogenisation with optimal segmentation and ANOVA correction: past, present and future. Proceedings of the ninth seminar for homogenization and quality control in climatological databases and fourth conference on spatial interpolation techniques in climatology and meteorology, Budapest, Hungary, 03 – 07 April 2017, WMO Climate Data and Monitoring report WCDMP-No. 85.

Domonkos P, Venema V, Mestre O. 2013. Efficiencies of homogenisation methods: our present knowledge and its limitation. Proceedings of the Seventh seminar for homogenization and quality control in climatological databases, Budapest, Hungary, 24 – 28 October 2011, WMO report, Climate data and monitoring, WCDMP-No. 78: 11-24.

Ducré-Robitaille J-F, Vincent LA, and Boulet G. 2003. Comparison of techniques for detection of discontinuities in temperature series. Int. J. Climatol., 23: 1087–1101.

Dunn RJH, Willett KM, Morice CP, and Parker DE. 2014. Pairwise homogeneity assessment of HadISD. Clim. Past, 10: 1501-1522, doi: 10.5194/cp-10-1501-2014.

Easterling DR and Peterson TC. 1995. A new method for detecting undocumented discontinuities in climatological time series. Int. J. Climatol., 15: 369–377.

Killick R. 2016. Benchmarking the Performance of Homogenisation Algorithms on Daily Temperature Data. PhD Thesis, Open Research Exeter, University of Exeter, UK.

Kuglitsch FG, Auchmann R, Bleisch R, Brönnimann S, Martius O, and Stewart M. 2012. Break detection of annual Swiss temperature series. J. Geophys. Res., 117: D13105, doi: 10.1029/2012JD017729.

Lindau R and Venema VKC. 2013. On the multiple breakpoint problem and the number of significant breaks in homogenization of climate records. Idöjaras - Quarterly Journal of the Hungarian Meteorological Service, 117, No. 1: 1–34.

Lindau R and Venema VKC. 2016. The uncertainty of break positions detected by homogenization algorithms in climate records. Int. J. Climatol., 36, No. 2: 576–589, doi: 10.1002/joc.4366.

Menne MJ and Williams CN. 2005. Detection of Undocumented Changepoints Using Multiple Test Statistics and Composite Reference Series. J. Climate, 18: 4271–4286, https://doi.org/10.1175/JCLI3524.1.

Menne MJ, Williams CN Jr., and Palecki MA. 2010. On the reliability of the US surface temperature record, J. Geophys. Res. Atmos., 115: D11108, doi: 10.1029/2009JD013094.

Parker DE. 1994. Effects of changing exposure of thermometers at land stations. Int. J. Climatol., 14: 1–31.

Peterson TC, Easterling DR, Karl TR, Groisman P, Nicholls N, Plummer N, Torok S, Auer I, Boehm R, Gullett D, Vincent L, Heino R, Tuomenvirta H, Mestre O, Szentimrey T, Salingeri J, Førland EJ, Hanssen-Bauer I, Alexandersson H, Jones P, and Parker D. 1998. Homogeneity adjustments of in situ atmospheric climate data: A review. Int. J. Climatol., 18: 1493–1517.

Trewin B. 2010. Exposure, instrumentation, and observing practice effects on land temperature measurements, WIREs Clim. Change, 1: 490–506, doi: 10.1002/wcc.46.

Venema V, Mestre O, Aguilar E, Auer I, Guijarno JA, Domonkos P, Vertacnik G, Szentimrey T, Stepanek P, Zahradnicek P, Viarre J, Muller-Westermeier G, Lakatos M, Williams CN, Menne MJ, Lindau R, Rasol D, Rustemeier E, Kalokythas K, Marinova T, Andresen L, Acquaotta F, Fratianni S, Cheval S, Klancar M, Brunetti M, Gruber C, Prohom Duran M, Likso T, Esteban P, and Brandsma T. 2012. Benchmarking homogenization algorithms for monthly data. Clim. Past, 8: 89–115.

Williams CN, Menne MJ, and Thorne PW. 2012. Benchmarking the performance of pairwise homogenization of surface temperatures in the United States. J. Geophys. Res., 117: D05116, doi: 10.1029/2011JD016761.

Appendix A: Correcting inhomogeneities in climate series with an ANOVA-type method

Consider an n x m matrix of observations $O(i,j)$ consisting of i = 1 to n time series with length j = 1 to m. The observations are fit to a linear model given by the two variables $C(j)$ and $B(i,j)$, where $C(j)$ denote the time dependent climate signal, which is considered to be identical at each station. The second variable $B(i,j)$ is the inhomogeneity for each station and year, which is considered to be constant over each homogenous subperiod (*HSP*) h = 1 to H between the two adjacent break points of a station. The position of the break points are known so that we can address a specific inhomogeneity, $B(i,j)$, alternatively as one-dimensional vector $B(h)$, with known $j_1(h)$ and $j_2(h)$ denoting the first and last year of the inhomogeneity, and $i_0(h)$ denoting the station it belongs to.

The observations are equal to a sum of three terms: The climate signal, the station inhomogeneity, and a random noise variable $\varepsilon(i,j)$:

$$O(i,j) = C(j) + B(i,j) + \varepsilon(i,j) \qquad (A1)$$

The noise, i.e. the square difference between model and observation, is minimized:

$$\sum_{i=1}^{n}\sum_{j=1}^{m}\big(C(j) + B(i,j) - O(i,j)\big)^2 = \min \qquad (A2)$$

$C(j)$ and $B(i,j)$ are unknowns to be determined. We perform the derivation of Eq. (A2) with respect to all of these unknowns and obtain $m+H$ equations for an equal number of unknowns. The derivations with respect to a fixed, but arbitrary $C(j)$ yield:

$$2\sum_{i=1}^{n}\big(C(j) + B(i,j) - O(i,j)\big) = 0 \qquad (A3)$$

which can be transformed to:

$$C(j) = \frac{1}{n}\sum_{i=1}^{n}\big(O(i,j) - B(i,j)\big) \qquad (A4)$$

In this way we have a number of m equations, one for each $C(j)$. Analogously, we derive Eq. (A2) with respect to the inhomogeneities $B(h)$. For a given, but arbitrary $B(h)$, it follows:

$$2\sum_{j=j_1(h)}^{j_2(h)}\big(C(j) + B(h) - O(i_0(h),j)\big) = 0 \qquad (A5)$$

where $j_1(h)$ and $j_2(h)$ denote the first and the last year of the considered HSP with length $l(h)$ and $i_0(h)$ the station it belongs to. Analogously to Eq. (A4), we can transform and solve for $B(h)$:

$$B(h) = \frac{1}{l(h)}\sum_{j=j_1(h)}^{j_2(h)}\big(O(i_0(h),j) - C(j)\big) \qquad (A6)$$

We obtain H equations, one for each of the inhomogeneities. According to Eq. (A6), a specific $B(h)$ is equal to the mean difference between the observations of the considered station i_0 and the climate signal C averaged over the duration of the HSP. The total number of $m+H$ equations (Eqs. (A4) and (A6)) can be reduced in two ways. Either we insert Eq. (A6) into Eq. (A4) and obtain m equations for the climate signal $C(j)$; or we insert vice versa Eq. (A4) into Eq. (A6) and obtain H equations for the inhomogeneities $B(h)$. The latter alternative yields:

$$B(h) = \frac{1}{l(h)} \sum_{j=j_1(h)}^{j_2(h)} \left(O(i_0(h), j) - \frac{1}{n} \sum_{i=1}^{n} \big(O(i,j) - B(i,j) \big) \right) \tag{A7}$$

Finally, we separate the inhomogeneities B from the observations O:

$$B(h) - \frac{1}{n\, l(h)} \sum_{j=j_1(h)}^{j_2(h)} \sum_{i=1}^{n} B(i,j) = \frac{1}{l(h)} \sum_{j=j_1(h)}^{j_2(h)} O(i_0(h), j) - \frac{1}{n\, l(h)} \sum_{j=j_1(h)}^{j_2(h)} \sum_{i=1}^{n} O(i,j) \tag{A8}$$

In Eq. (A8) we consider a specific inhomogeneity $B(h)$ occurring at station i_0 during the period j_1 to j_2. The double summation on the left-hand side gives the average over the inhomogeneities of all stations in that period. The difference between the candidate and the average of all stations is relevant. An analogous difference stands on the right-hand side of Eq. (A8). This expression is known and can be calculated from the observations. The interpretation of Eq. (A8) is as following: Inhomogeneities are detectable by anomalies in the observations compared to the average of neighbor stations during the same period. As always differences of identical periods are considered, the climate effect is cancelled out. However, the inhomogeneities are still mutually dependent.

We multiply Eq. (A8) by n and $l(h)$ to avoid fractional numbers in the following calculations:

$$n\, l(h) B(h) - \sum_{j=j_1(h)}^{j_2(h)} \sum_{i=1}^{n} \big(B(i,j) \big) = n \sum_{j=j_1(h)}^{j_2(h)} \big(O(i_0(h), j) \big) - \sum_{j=j_1(h)}^{j_2(h)} \sum_{i=1}^{n} \big(O(i,j) \big) =: O'(h) \tag{A9}$$

The known right-hand side expression is combined and called $O'(h)$. The number of overlapping years $L(h,hh)$ between the candidate inhomogeneity $B(h)$ and those from neighboring stations $B(hh)$ are crucial in Eq. (A9). Using the overlapping information $L(h,hh)$,we can rewrite Eq. (A9):

$$n\, l(h)\, B(h) - \sum_{hh=1}^{H} L(h,hh)\, B(hh) = O'(h) \tag{A10}$$

Considering all H equations together, we can write them in matrix form:

$$\overline{\overline{M}} \cdot \overrightarrow{B} = \overrightarrow{O'} \tag{A11}$$

The diagonal of the matrix **M** is given by:

$$M(h,h) = (n-1)\, l(h) \tag{A12}$$

which can be deduced by setting $hh = h$ in Eq. (A10) and using the identity $L(h,h) = l(h)$. The non-diagonal elements are equal to the negative of the number of overlapping years:

$$M(h, hh) = -L(h, hh) \quad for\ h \neq hh \tag{A13}$$

Fig. A1 shows an example with five stations containing two breaks each so that 15 HSP exist. The corresponding inhomogeneities are numbered from $B1$ to $B15$. In the upper panel, $B8$ is chosen as candidate. In brackets the number of overlapping years with $B8$ is given: $L(8,i)$.

M is a sparse matrix, i.e. many entries are zero, because many HSPs do not overlap. As the overlap of two HSPs is mutually equal, M is symmetric. A further characteristic is that the sum of all elements in one row (or column) is equal to zero, because the sum of all non-diagonals is equal with opposite sign to the diagonal element (n-1 stations times $l(h)$, the length of the considered HSP). Therefore, the solution is not unique: Adding an arbitrary constant to a specific solution vector $B(h)$ is also a solution. Thus, the mean over all inhomogeneities is not determinable, but that is irrelevant for the trend.

Information about the position of the breaks is used to compute the Matrix M. Assuming a pure break signal without noise, errors in the break positions may lead to an error variance of the inhomogeneities B in the order of the break variance itself, if true and predicted break positions are completely uncorrelated. However, even if the detection is completely correct, there is a minimum error variance caused by the noise ε. In this situation the error variance of the estimated break signal is equal to the spuriously explained variance of a pure noise time series by random breaks. Lindau and Venema (2013) showed that this variance is equal to $k/(m\text{-}1)\ \sigma_n^2$, where k denotes the number of breaks and m the length of the time series. Thus, an estimate for the minimum error variance of the inhomogeneities, occurring even if the break detection is perfect, is:

$$\overline{\Delta B \Delta B} \;=\; \frac{k}{m-1}\,\sigma_n{}^2 \tag{A14}$$

Appendix B: Number of independents for the step function of an inhomogeneity signal

Consider a time series that is generated by choosing *m* random numbers from a standard normal distribution with zero mean. A fraction of (*m*-1)/*m* of the input variance can be found as internal variance in the obtained time series, whereas the rest (1/*m*) arise as external variation of the temporal means of each times series. (This is the reason why we have to divide by *m*-1, when we want to estimate the variance of a sample). It is a commonly known feature that the factor of variance reduction attained by averaging is equal to the number of independents in the sample and in the above example all *m* values are independent.

Consider now a time series of inhomogeneities (again with random and normal distributed deviations from zero). Such a time series contains obviously less independent values. It consists of only a few constant subperiods interrupted by jumps at the *k* breakpoints. The temporal mean of such a time series is given by the weighted mean:

$$\bar{x} = \frac{1}{m}\sum_{i=1}^{k+1} l_i x_i \qquad (B1)$$

where l_i denote the length and x_i the value of each homogeneous subperiod. The external variance is:

$$Var(\bar{x}) = [\bar{x}\bar{x}] = \left[\left(\frac{1}{m}\sum_{i=1}^{k+1} l_i x_i\right)^2\right] = \frac{1}{m^2}\sum_{i=1}^{k+1}\sum_{j=1}^{k+1}[l_i l_j x_i x_j] \qquad (B2)$$

where the square brackets denote the expected value: $[\bar{x}]$ is zero, which allows for the first equal sign in Eq. (B2).

As *x* is a random variable all mixed terms of *i* and *j* in Eq. (B2) become zero; further we can separate averages over x_i^2 and l_i^2 from each other as *x* and *l* are independent; and because the variance of *x* is 1, we can finally write:

$$Var(\bar{x}) = \frac{1}{m^2}\sum_{i=1}^{k+1}[l_i^2 x_i^2] = \frac{1}{m^2}\sum_{i=1}^{k+1}[l_i^2][x_i^2] = \frac{1}{m^2}\sum_{i=1}^{k+1}[l_i^2] \qquad (B3)$$

If the *k*+1 subperiods have all the same length *l*, the external variance amounts to:

$$Var(\bar{x}) = \frac{l^2}{m^2}\sum_{i=1}^{k+1} 1 = \frac{l^2}{m^2}(k+1) \qquad (B4)$$

For equal lengths $l = m/(k+1)$ and it follows:

$$Var(\bar{x}) = \frac{1}{k+1} \qquad (B5)$$

If the lengths are constant, averaging over a time series of *k*+1 homogeneous subperiods reduces the variance by the same factor, as *k*+1 is not only the nominal, but also the effective number of independents.

However, in the real world the lengths of inhomogeneities are variable. If a 100-year time series consists of a 96-year inhomogeneity and 4 further one year long ones, it is obvious that the effective number of independents must be smaller than 5. The variance of such time series means will be closer to 1 than to 1/5.

We restart our considerations for variable lengths with Eq. (B3). First, except for edge effects, the mean square length is the same for all *k* subperiods. With this approximation it follows:

$$Var(\bar{x}) \;=\; \frac{k+1}{m^2}\,[l^2] \qquad (B6)$$

Eq. (B6) shows that we need to know the mean square length of the inhomogeneities, which can be concluded from the frequency distribution of lengths. There are $\binom{m-1}{k}$ possibilities to distribute *k* breaks in a time series of length *m*. The relative frequency of a subperiod's length is then given by:

$$p(l) \;=\; \frac{\binom{m-l-1}{k-1}}{\binom{m-1}{k}} \qquad (B7)$$

The nominator of Eq. (B7) gives the total number of possibilities for a given length *l*, while the denominator gives the total number of combinations. The nominator of Eq. (B7) becomes plausible by the following consideration. We have *k* breaks (generating *k*+1 subperiods) within a time series of length *m*. If a subperiod has the length *l*, the remaining part (of length *m-l*) has to be shared by *k* subperiods. Thus, we have to put *k*-1 breaks into a time series of length *m-l*. There are $\binom{m-l-1}{k-1}$ different possibilities to do so.

We further see that $l = m - k$ is the maximum length for a subperiod, because this leaves just enough space for the other *k* subperiods. Expressing the mean over l^2 as the frequency weighted sum and inserting the maximum length as upper summation limit, we can rewrite Eq. (B6):

$$Var(\bar{x}) \;=\; \frac{k+1}{m^2}\sum_{l=1}^{m-k} p(l)\, l^2 \qquad (B8)$$

Inserting Eq. (B7) into (B8) we get:

$$Var(\bar{x}) \;=\; \frac{k+1}{m^2}\,\frac{1}{\binom{m-1}{k}}\sum_{l=1}^{m-k}\binom{m-l-1}{k-1} l^2 \qquad (B9)$$

The sum in Eq. (B9) can be solved by applying the following identity:

$$\sum_{l=0}^{m}\binom{l}{j}\binom{m-l}{k-j} \;=\; \binom{m+1}{k+1} \qquad (B10)$$

Using the solutions for *j* = 1 and *j* = 2, it follows:

$$\sum_{l=1}^{m-k}\binom{m-l-1}{k-1} l^2 \;=\; \frac{2m-k}{k+2}\,\binom{m}{k+1} \qquad (B11)$$

Inserting Eq. (B11) into (B9) we obtain:

$$Var(\bar{x}) = \frac{k+1}{m^2} \frac{1}{\binom{m-1}{k}} \frac{2m-k}{k+2} \binom{m}{k+1} \qquad (B12)$$

The two binomial coefficients can be expressed as one quotient:

$$Var(\bar{x}) = \frac{k+1}{m^2} \frac{m}{k+1} \frac{2m-k}{k+2} \qquad (B13)$$

Finally we get:

$$Var(\bar{x}) = \frac{2m-k}{m\,(k+2)} \qquad (B14)$$

For $m \gg k > 1$ we can further approximate:

$$Var(\bar{x}) \approx \frac{2}{(k+2)} \qquad (B15)$$

The number of independents is equal to the reciprocal of the result in Eq. (B15):

$$m_{in} \approx \frac{k}{2} + 1 \qquad (B16)$$

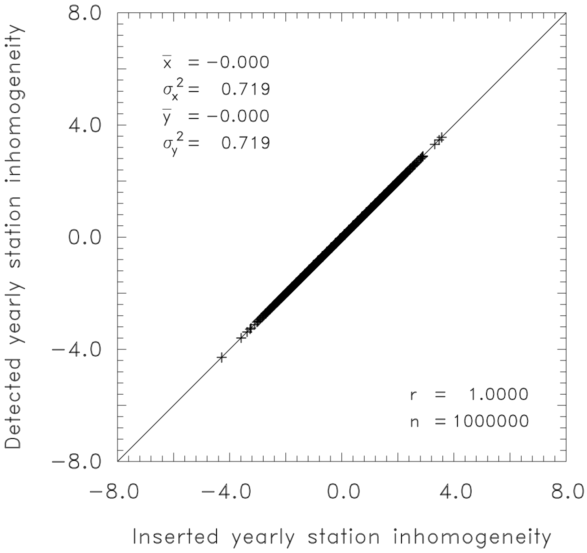

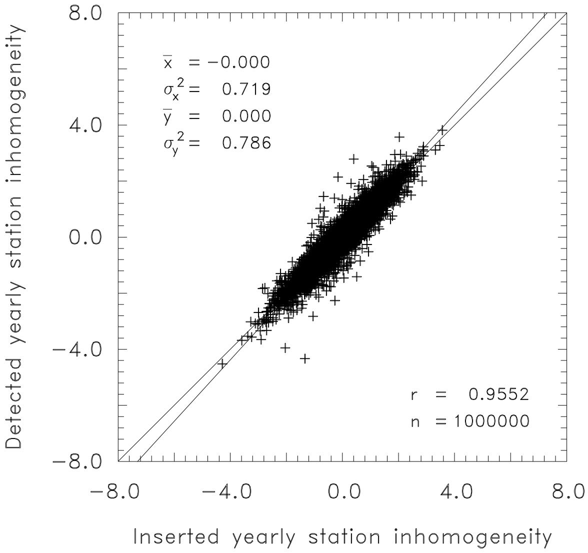

Fig. 1: Simulation of 1000 networks consisting of 10 stations with 5 breaks each, with known break positions, the break variance is set to 1 and the noise variance to zero. The correction scheme works perfectly. $\bar{x}$ and $\bar{y}$ give the means of the two compared parameters, ${\sigma_x}^2$and ${\sigma_y}^2$ their variances, *r* their correlation, and *n* the number of samples.

Fig. 2a: As Fig. 1, but both break and noise variance is set to 1. The panel shows the situation after the first step, the correction itself. Each cross denotes the inserted and the detected inhomogeneity for 1000 networks, with 10 stations and 100 years.

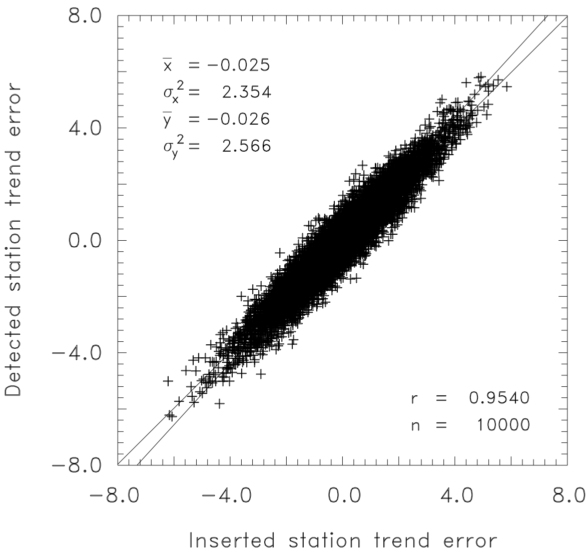

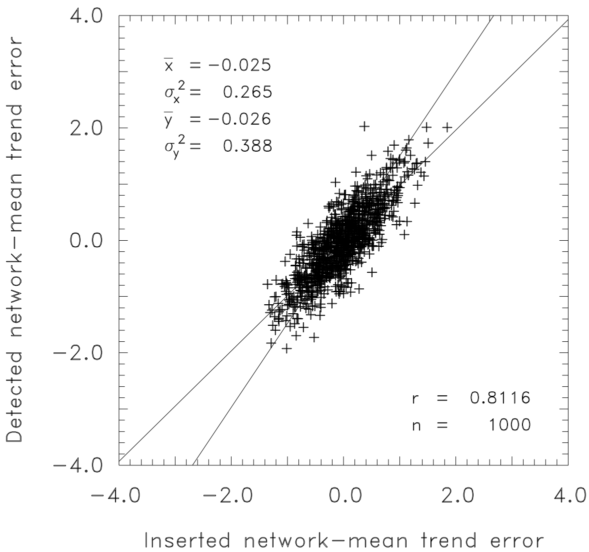

Fig. 2b: As Fig. 2a, but after the second step, i.e. for station trends. Each cross denotes the inserted and detected trend for 1000 networks with 10 stations.

Fig. 2c: As Fig. 2a, but after the third step, i.e. for network trends. Each cross denotes the inserted and detected network-mean trend for 1000 networks.

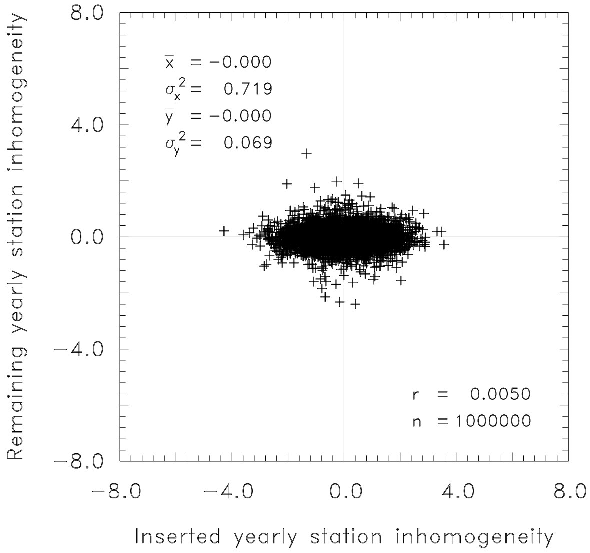

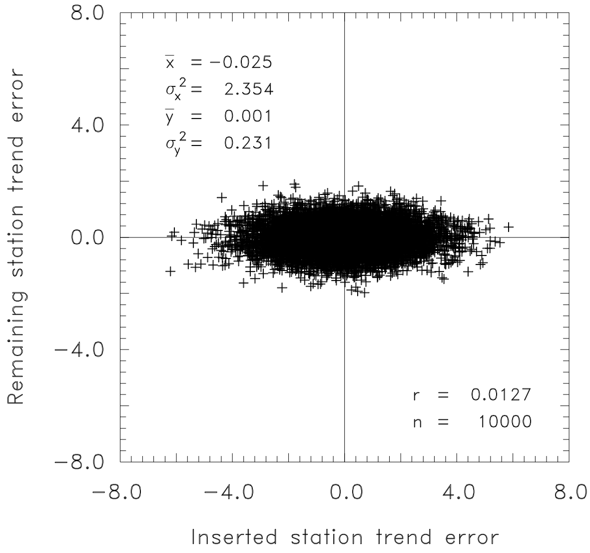

Fig. 3a: As Fig. 2a, but for the remaining inhomogeneities instead of the detected ones.

Fig. 3b: As Fig. 2b, but for the remaining station trends instead of the detected ones

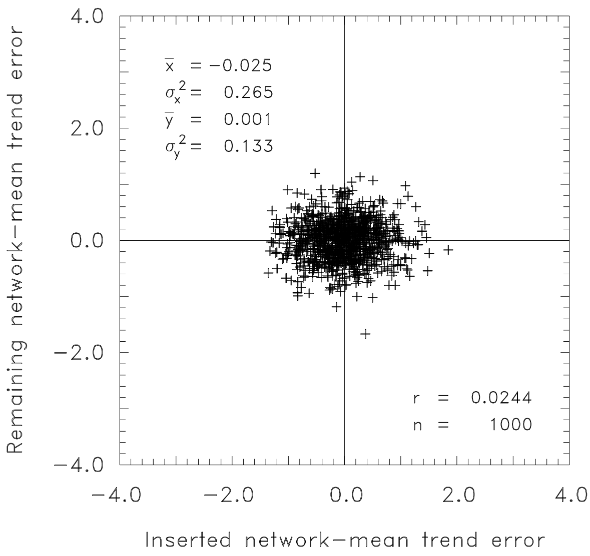

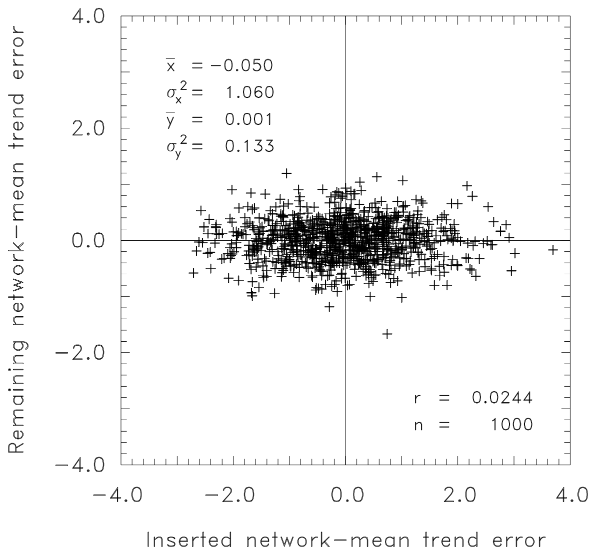

Fig. 3c: As Fig. 2c, but for the remaining network-mean trends instead of the detected ones. This is the result for **Scenario 1** assuming unbiased break sizes and correct positions.

Fig. 4: As Fig 3c, but the standard deviation of the inserted breaks is increased from 1 to 2, while the standard deviation of the noise remains at 1.

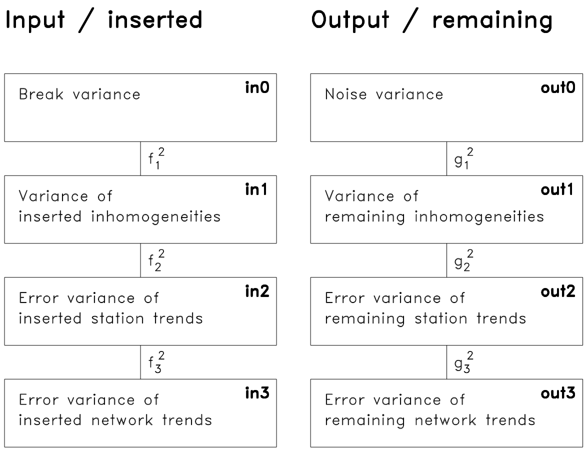

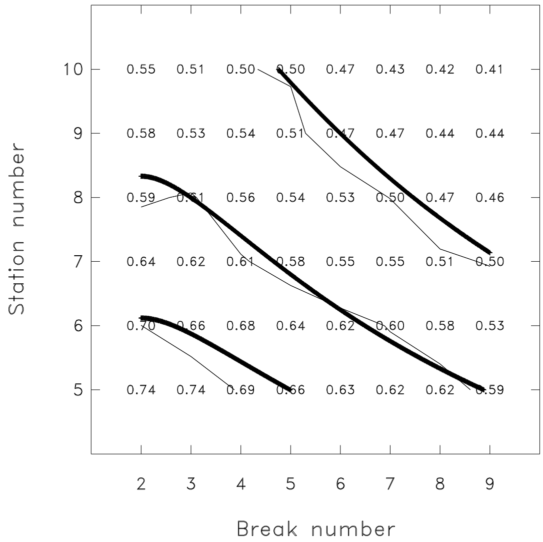

Fig. 5: Flowchart for the input (left) and output (right) variables as they are given in Fig. 3 on the x- and y-axis, respectively. The transitions of the input states in0 to in3 are given by the factors f_1^2 to f_3^2, that of the output states by the factors g_1^2 to g_3^2.

Fig. 6a: The factor *f* as a function of break and station number. Three isolines are drawn for *f* = 0.5, 0.6, and 0.7. The theoretical values from Eq. (17) are given as fat isolines for the same three values.

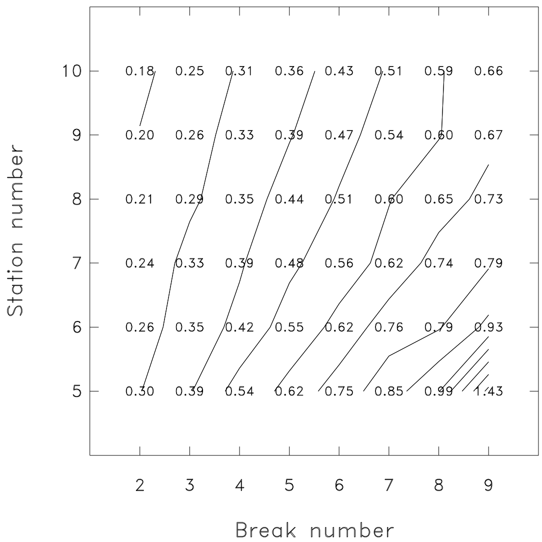

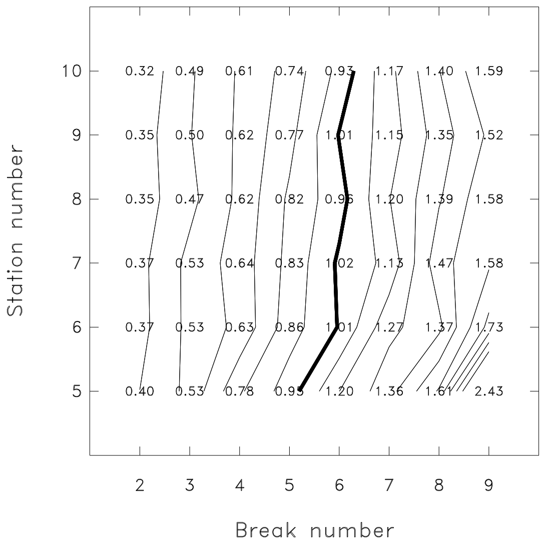

Fig. 6b: The factor *g* as a function of break and station number. Isolines are drawn for *g* = 0.2 to 1.4 in steps of 0.1.

Fig. 6c: The factor *g*/*f* as a function of break and station number. Isolines are drawn for *g*/*f* = 0.4 to 2.0 in steps of 0.1. The line g/f = 1 is drawn fat.

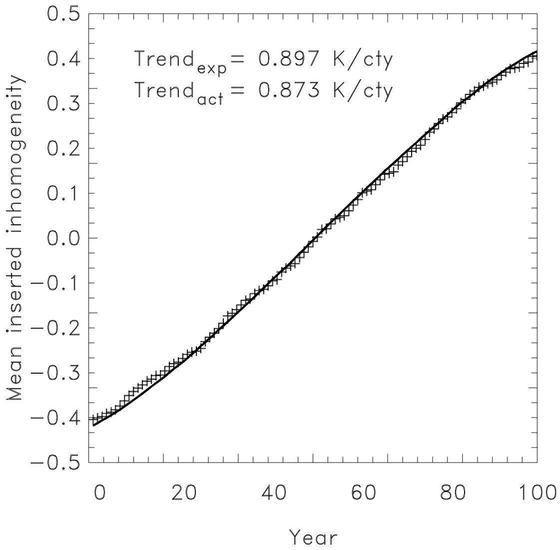

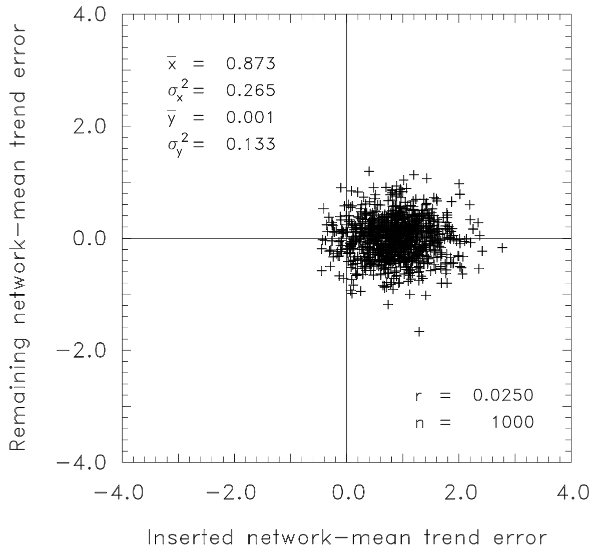

Fig. 7: The mean inserted inhomogeneity for a bias according to Eq. (20) is given by the fat line. Due to edge effects the introduced trend is decreased from 1 to 0.897 K /cty. If additionally random breaks with $\sigma_b = 1$ are included, the actually inserted trend is scattered and differs slightly with 0.873 K/cty.

Fig. 8: As Fig. 3c, but with an additionally inserted trend bias of 0.873 K/cty as depicted in Fig. 7. This is the result for **Scenario 2** assuming biased break sizes and correct positions.

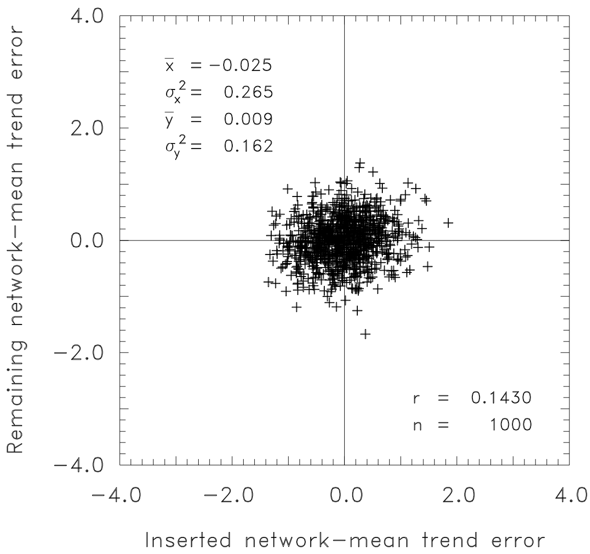

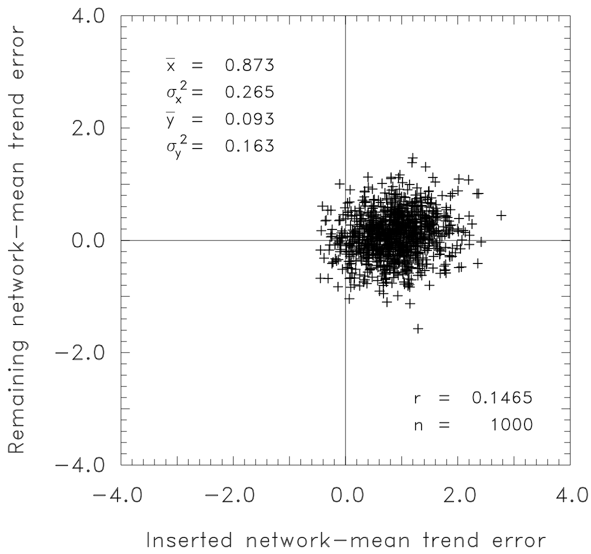

Fig. 9: As Fig. 3c, but assuming additionally a position error of $\sigma_s = 1$. This is the result for **Scenario 3** assuming unbiased break sizes and perturbed positions.

Fig. 10: As Fig. 8, but assuming additionally a position error of $\sigma_s = 1$. This is the result for **Scenario 4** assuming biased break sizes and perturbed positions.

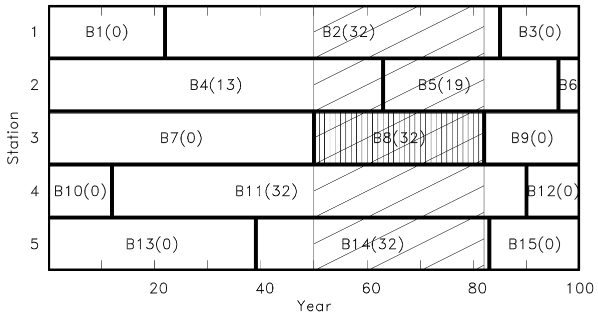

$$
\begin{matrix}
88 & 0 & 0 & -22 & 0 & 0 & -22 & 0 & 0 & -12 & -10 & 0 & -22 & 0 & 0 \\
0 & 252 & 0 & -41 & -22 & 0 & -28 & -32 & -3 & 0 & -63 & 0 & -17 & -44 & -2 \\
0 & 0 & 60 & 0 & -11 & -4 & 0 & 0 & -15 & 0 & -5 & -10 & 0 & 0 & -15 \\
-22 & -41 & 0 & 252 & 0 & 0 & -50 & -13 & 0 & -12 & -51 & 0 & -39 & -24 & 0 \\
0 & -22 & -11 & 0 & 132 & 0 & 0 & -19 & -14 & 0 & -27 & -6 & 0 & -20 & -13 \\
0 & 0 & -4 & 0 & 0 & 16 & 0 & 0 & -4 & 0 & 0 & -4 & 0 & 0 & -4 \\
-22 & -28 & 0 & -50 & 0 & 0 & 200 & 0 & 0 & -12 & -38 & 0 & -39 & -11 & 0 \\
0 & -32 & 0 & -13 & -19 & 0 & 0 & 128 & 0 & 0 & -32 & 0 & 0 & -32 & 0 \\
0 & -3 & -15 & 0 & -14 & -4 & 0 & 0 & 72 & 0 & -8 & -10 & 0 & -1 & -17 \\
-12 & 0 & 0 & -12 & 0 & 0 & -12 & 0 & 0 & 48 & 0 & 0 & -12 & 0 & 0 \\
-10 & -63 & -5 & -51 & -27 & 0 & -38 & -32 & -8 & 0 & 312 & 0 & -27 & -44 & -7 \\
0 & 0 & -10 & 0 & -6 & -4 & 0 & 0 & -10 & 0 & 0 & 40 & 0 & 0 & -10 \\
-22 & -17 & 0 & -39 & 0 & 0 & -39 & 0 & 0 & -12 & -27 & 0 & 156 & 0 & 0 \\
0 & -44 & 0 & -24 & -20 & 0 & -11 & -32 & -1 & 0 & -44 & 0 & 0 & 176 & 0 \\
0 & -2 & -15 & 0 & -13 & -4 & 0 & 0 & -17 & 0 & -7 & -10 & 0 & 0 & 68
\end{matrix}
$$

Fig. A1: Sketch to illustrate the setup of the matrix (lower panel) that has to be solved for the ANOVA correction. The example considers five stations with altogether 15 HSPs. The circumstances for the 8[th] inhomogeneity (dark shaded) are given exemplarily in the upper panel. Crucial are the overlapping periods (light shaded), the length of which are additionally given in brackets for each HSP. These numbers occur with a negative sign in line 8 of the matrix *M*, which is shown in the lower panel. In this example, the diagonal element of line 8 is equal to 128 according to Eq. (A12) for n = 5 and $l(h)$ = 32.

Tab. 1: Summary of the different experiments. In all experiments 1000 simulated networks are analyzed consisting of 10 time series of length 100 with 5 breakpoints each. Six setting parameters are varied: the standard deviations of breaks and noise, σ_b and σ_n, respectively; the decision whether the detected (*D*) or remaining (*R*) error is considered and which of the three correction steps. Further the considered scenario, i. e. whether the break positions are perturbed (given as standard deviation σ_s) and whether biased or unbiased breaks are assumed. The results are also given by six values: Mean and standard deviation of input ($\bar{x}$ and σ_x) and output ($\bar{y}$ and σ_y) of the correction procedure, their correlation *r* and the total number of samples *N*.

	Settings						Results					
Figure	σ_b	σ_n	*D/R*	step	σ_s	biased	$\bar{x}$	σ_x^2	$\bar{y}$	σ_y^2	*r*	*N*
1	0	1	D	1	0	no	0.0	0.719	0.0	0.719	1.000	10^6
2a	1	1	D	1	0	no	0.0	0.719	0.0	0.786	0.955	10^6
2b	1	1	D	2	0	no	0.0	2.354	0.0	2.566	0.954	10^4
2c	1	1	D	3	0	no	0.0	0.265	0.0	0.388	0.812	10^3
3a	1	1	R	1	0	no	0.0	0.719	0.0	0.069	0.005	10^6
3b	1	1	R	2	0	no	0.0	2.354	0.0	0.231	0.013	10^4
3c	1	1	R	3	0	no	0.0	0.265	0.0	0.133	0.024	10^3
4	2	1	R	3	0	no	0.0	1.060	0.0	0.133	0.024	10^3
not shown	1	2	R	3	0	no	0.0	0.265	0.0	0.531	0.024	10^3
8	1	1	R	3	0	yes	0.873	0.265	0.0	0.133	0.025	10^3
9	1	1	R	3	1	no	0.0	0.265	0.0	0.162	0.143	10^3
not shown	1	1	R	3	2	no	0.0	0.265	0.0	0.203	0.218	10^3
10	1	1	R	3	1	yes	0.873	0.265	0.093	0.163	0.147	10^3
not shown	1	1	R	3	2	yes	0.873	0.265	0.180	0.208	0.220	10^3